TORSIONAL VIBRATION IN PUMP/DRIVER SHAFT TRAINS THE ROLE OF EXTERNAL DAMPING FROM PUMP IMPELLERS

by

Rainer Nordmann

Professor of Machine Dynamics and Control Theory

University of Kaiserslautern

Kaiserslautern, Germany

Peter Weiser

Head, Mechanical Design and Development

Komeg Presicion Parts and Metrology

Völklingen, Germany

Arno Frei

Manager Mechanical Development

and

Rudolf Stuerchler

Sulzer Brothers, Ltd. Pump Division

Winterthur, Switzerland

Rainer Nordmann completed his doctoral degree (Mechanical Engineering) in 1974 at the Technical University of Darmstadt in Germany. He was assistant Professor at Machine Dynamics Institute and became head of the Dynamics Laboratory in 1976. Since 1980, he has been Professor of Machine Dynamics and Control Theory at the University of Kaiserslautern. His research group includes 12 research assistants and 15 student research assistants. In the past 12 years, about 30 research projects have been carried out in the areas of rotordynamics, identification techniques, modal analysis, simulation techniques, bearing and seal dynamics, active magnetic bearings and diagnosis. Funding for this research is from the Government, the European Community and from companies. Dr. Nordmann has published 80 papers.

Peter Weiser received an M. Sc. degree (Mechanical Engineering) from the University of Kaiserslautern, Germany (1985). From 1985-1990, he did research work for torsional damping effects in centrifugal pumps at the laboratories of the University of Kaiserslautern and under contract of Sulzer Pump Division, while he worked on his Ph.D. thesis. He has been Research Engineer in Völklingen, Germany since 1991. Dr. Weiser is Head of the Mechanical Design and Development Department.

Arno Frei graduated (1959) from St. Gall Technical College, Switzerland, with a degree (Mechanical Engineering). He joined Sulzer in 1966 and was first engaged in the design and development of primary recirculation pumps for nuclear power stations. After activities in the field of nuclear heat exchangers, he rejoined the pump division, where he has been Head of the Mechanical Development Group since 1978. Activities of the group include rotordynamics, structural dynamics, finite element thermal and stress analysis, pump component development, and tribology.

ABSTRACT

Consideration of torsional vibration in pump/driver shaft trains has become of increasing importance with the development of electronically controlled variable speed electric motors. Such motors not only provide a static driving torque, but develop superimposed continuous torque pulsations. The frequency of these torque pulsations varies with speed, such that typically resonance situations with a torsional natural mode at distinct speeds cannot be avoided. Whether such resonance situations can be sustained during extended time periods without endangering the shafts by fatigue depends primarily on the total amount of damping available in the shaft train. Besides material and structural damping, which are internal damping sources, pump impellers are expected to provide external damping by convective energy dissipation into the pumped fluid. From literature, predictions of impeller damping on a theoretical basis are known, but almost no information about an experimental identification of torsional damping coefficients is available.

The authors describe the development of a test rig for the identification of torsional damping and added mass moment of inertia of pump impellers. To find a suitable method to excite the test shaft train within a sufficiently large frequency band was the main difficulty to solve when developing the test rig. Test results are shown and compared with theoretical predictions. Application on an installation with a variable speed motor is described and conclusions with respect to shaft safety against fatigue are drawn.

INTRODUCTION

In the past, little attention has been paid by the designers to the torsional behavior of pump shaft trains. Asynchronous three phase motors, which are the common drivers of constant speed pumps, deliver a smooth driving torque, with almost no pulsating dynamic component, during normal operation. At startup, when the motor is switched to the grid, it has been well known that impact-like transient dynamic torque variations take place [1], with normally no severe consequences for the shaft train. This is due to the fact that the mass moment of inertia of the pump rotor is typically much smaller than that of the motor rotor. The dynamic torque transmitted by the coupling from the motor to the pump rotor is therefore considerably smaller than the dynamic airgap torque, provided no resonance between line frequency and one of the torsional natural modes takes place.

However, in shaft trains with a speed increasing gear between motor and pump, sliding in the shrink fit between gear wheel and shaft has been experienced during startup.

Variable speed pumpsets have either been equipped with turbines as a driver or with turbocouplings driven by a constant speed electric motor. Such driver systems produce almost no dynamic torque; at least on the pump side in case of a turbocoupling.

Within the last decade, motor manufacturers have brought variable speed alternating current motors on the market. During normal operation, these motors not only develop a static torque, but show superimposed dynamic torque pulsations. The frequency of these torque pulsations is a function of shaft speed [2]. Hence, the designer is faced with resonance between excitation frequencies and torsional natural frequencies, which can occur during extended time periods. Safety against fatigue failure becomes a major issue. At resonance, the important parameters influencing the dynamic torque transmitted from the motor to the pump shaft are:

- The amplitude of the dynamic airgap torque.
- The torsional damping available in the shaft train.

It is here where the torsional damping is of major concern. Torsional damping in a shaft train can be classified as follows:

Internal Damping

- Material damping
- in the steel parts of the shaft train
- in the elastomeric elements of damper couplings
- Structural damping
- at mating surfaces of rotor parts

External damping

- Damping through the surrounding medium

Critical damping ratios of natural modes due to internal damping, without the use of damper couplings, are typically in a range between one and two percent [3]. The question arises how far the damping will be raised by external impeller damping. Literature describing theoretical investigations on impeller damping is available [5, 6].

However, no work treating the experimental identification is known to the authors.

It was therefore decided to build a testrig for this purpose.

TORSIONAL EXCITATION AND THE ROLE OF TORSIONAL DAMPING IN PUMP SHAFT TRAINS

Torsional excitation in pump shaft trains arises mainly in the driver and in gears. The most important excitations are listed in Table 1. Excitation from the impellers can be neglected if the vane number combination impeller/diffuser is selected properly [7].

Table 1. Torsional Exciation Mechanisms in Pump Shaft Trains.

Source of excitation	Condition	Excit. Freq. [Hz]	Excitation Torque	Remarks, Explanations
Asynchronous electric motor	Line start	f_F	$M(t) = M_0 + M_1 e^{-\frac{t}{T}} \sin(2\pi f_F t)$	f_F = Stator feed freq.
Asynchronous or synchr. electric motor	Phase-to-phase short circuit	f_F, $2f_F$	$M(t) = M_K\{e^{\frac{t}{T_1}} \sin(2\pi f_F t) - 0.5 e^{-\frac{t}{T_2}} \sin(4\pi f_F t)\}$	f_F = Stator feed freq.
Variable speed asyn. motor, subsynchr. cascade controlled	Normal operation	$z \cdot s\, f_F$	$M(t) = \sum M_Z(n) \sin(zs2\pi f_F t)$	z = Harmonics no. typically 6, 12 s = slip = $\frac{n_{syn} - n}{n_{syn}}$ f_F = Stator feed freq. (constant)
Variable speed syn. motor, thyristor controlled	Normal operation	$z \cdot f_F$	$M(t) = \sum M_Z(n) \sin(z2\pi f_F t)$	z = Pulse number (6, 12, 18 ...) f_F = Variable stator feed frequency proportional to shaft speed
Constant speed synchronous motor	Asynchr. startup	f_F $2sf_F$	$M(t) = M_0 + M_1 e^{-\frac{t}{T}} \sin(2\pi f_F t) + M_2(n) \sin(2s2\pi f_F t)$	f_F = Stator feed freq. s = slip = $\frac{n_{syn} - n}{n_{syn}}$
Spur gear	Pinion pitch circle runout	$f = \frac{n_P}{60}$	$M(t) = M_P \sin(2\pi f t)$	n_P = Pinion speed [rpm] M_P = 0 ...1% of static pinion torque
	Gearwheel pitch circle runout	$f = \frac{n_{GW}}{60}$	$M(t) = M_{GW} \sin(2\pi f t)$	n_{GW} = Gearwheel speed [rpm] M_{GW} = 0...1% of static gearwheel torque
	Gear tooth meshing	$f = z_P \frac{n_P}{60} = z_{GW} \frac{n_{GW}}{60}$	$M(t) = M_{TM} \sin(2\pi f t)$	z_P = No of pinion teeth z_{GW} = No of gearwheel teeth

For a shaft train with motor, coupling, and pump excited by a dynamic airgap torque in the electric motor and damped by internal damping, the dynamic torque transmitted by the coupling between motor and pump shaft, writes Ehrich [4]:

$$M_{dyn,\,trans} = M_{dyn,\,airgap} \frac{\Theta_{pump}}{\Theta_{pump} + \Theta_{motor}} AF \qquad (1)$$

The amplification factor AF depends on

- the decay rate of the exciting airgap torque in case of a transient excitation like line starting of an electric motor.
- the separation margin between excitation frequencies and natural frequencies of the system.
- the damping available in the system.

As mentioned before, critical damping ratios ζ of natural modes due to internal damping are typically in a range between one and two percent [3]. For steady state dynamic excitation, this leads to amplification factors at resonance between 25 and 50.

$$AF = \frac{1}{2\zeta} \qquad (2)$$

Additional external damping will reduce the amplification factor. Theoretical investigations treating impeller damping are available [5, 6]. These investigations predict the impeller damping to be dominated by the quasisteady term.

Quasisteady means that the damping is of the same nature as the torque variation with shaft speed. In fact, a torsional vibration is nothing than a fast shaft speed fluctuation. The quasisteady damping coefficient of an impeller thus becomes

$$D = \frac{dM}{d\omega} \tag{3}$$

For a pump impeller, the torque varies quadratically with speed

$$M = C\,\omega^2 \tag{4}$$

Hence Equation (3) writes

$$D = 2C\omega. = \frac{2M}{\omega} = \frac{2P}{\omega^2} \tag{5}$$

According to Equation (5), the torsional damping coefficient is proportional to shaft speed. This equation is also given Vance [3] and Ehrich [4].

However, no publication treating the experimental identification of torsional impeller damping is known to the authors. The decision was therefore taken to build a test rig as described in the next section.

DEVELOPMENT OF A TEST RIG FOR THE IDENTIFICATION OF IMPELLER DAMPING AND ADDED MASS MOMENT OF INERTIA

To meet the practical demands for the measurement and proper interpretation of data for impeller damping and mass moment of inertia, the following keyrequirements for a successful design of a test rig were established:

- Avoidance of external influences on the test rig, e.g., floor vibration
- Decoupling of all important test parameters and separate controllability of all parameters
- Minimization of system components with clear definition of each component function

With these principles in mind, the following system components (Figure 1) and their associated tasks can be defined:

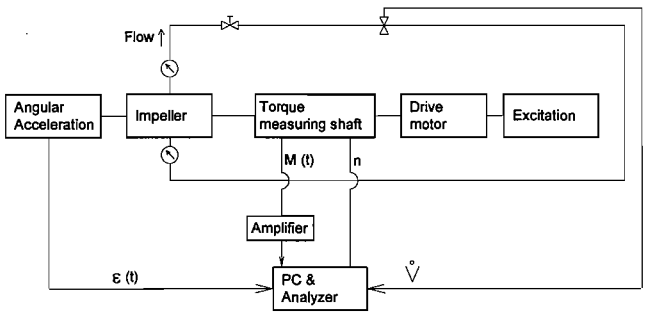

Figure 1. Test Rig Assembly.

- Test rig vibration isolation using visco-damped spring elements achieving strongly damped eigenmodes and low eigenfrequencies
- Test rig support structure consisting of a steel-welded construction being very stiff for torsional and bending modes of the whole test rig
- Closed-loop water circulation driven by the pump under test avoiding the necessity of a reservoir
- Throttle valve for the adjustment of mass flow and operating conditions
- Flow rectifier for achieving a homogeneous velocity profile of turbulent water flow
- Flow pressure measurement device for determination of exact mass flow
- 3-phase asynchronous electrical motor with Y-D run up control
- In-shaft torque measurement device between pump and drive motor
- Measurement device for the determination of angular acceleration
- Spectral analyzer for the determination of the impedance function and the extraction of the measurement results for impeller damping and mass moment of inertia.

Most of these components are standard elements and are, therefore, not explained in further detail, but two parts, which are the most important for the measurement procedure, will be the subject of further comments.

Excitation Systems

Excitating the system consisting of pump and drive motor during nearly constant running speed conditions is the most important but also the most difficult part of the work that had to be done. Normally, pump and motor are coupled via an appropriate coupling device. In this case, a torque measurement shaft is used to determine the time-varying torque acting between pump and motor. This is the physical input to the pump under test. The pump answers to this torsional excitation with angular acceleration being the output of the pump, where phase and amplitude are determined by the damping and mass characteristics due to the flow in impeller, seals and the surrounding fluid. To determine these damping and mass parameters, the system must be torsionally excited. The authors have decided to distinguish between excitation at no running speed and excitation mechanisms during the normal operational speed of the pump:

- At no running speed, the shaft was excited using an electromagnetic shaker which was coupled to the end of the drive motorís shaft via a mechanical coupling allowing no bending influences
- At normal operational speed, there are several possible excitation mechanisms, each having its own benefits and restrictions:

1) Manipulation of drive motor to generate transient torque
2) Rotating mass unbalance exciter
3) Impact during Y-Δ switching
4) Impact generation at free end of shaft using a brake
5) Sudden clutching of mass moment of inertia at free end of shaft train
6) Leonard-Ward-circuit as control device for a direct current electrical machine in the main shaft train.

While 1) offers a cheap method, but requiring detailed knowledge of the drive motor, 2) leads to a very complicated design and big problems in fulfilling several safety requirements, because large centrifugal forces are generated. The methods promising success under practical conditions are 3) and 4), because there is a low-cost and realistic possibility to excite the system by considerable forces in an acceptable frequency range. Method 5) allows only the excitation of the system at discrete frequencies determined through the mass moment of the disks to be clutched to the shaft train. At the very end, method 6) shows the possibilities in electrical drive theory, but the practical conclusion is, that this is at least a very cost-intensive way to go with many technical problems in designing an appropriate direct current machine.

Therefore, the authors first built a test rig excitation component following principle 4). Tests showed, that this method works well for low excitation frequencies, but at higher frequencies, the impact generated using a brake does not contain enough energy to excite the system. On the other hand, the Y-Δ-switching always causes a very sharp impact containing sufficient excitation energy even at relatively high frequencies. Therefore, the researchers adopted this method as our standard excitation mechanism.

Angular Acceleration Sensor

The device utilized is shown on Figure 2. Two acceleration probes are mounted on a disk 180 degrees apart. These probes measure acceleration in tangential direction. The above arrangement of probes has the advantage of doubling the sensitivity for tangential (and thus angular) accelerations, whereas lateral accelerations are fully compensated. Current supply and signal transmission are done via a mercury type transmitter.

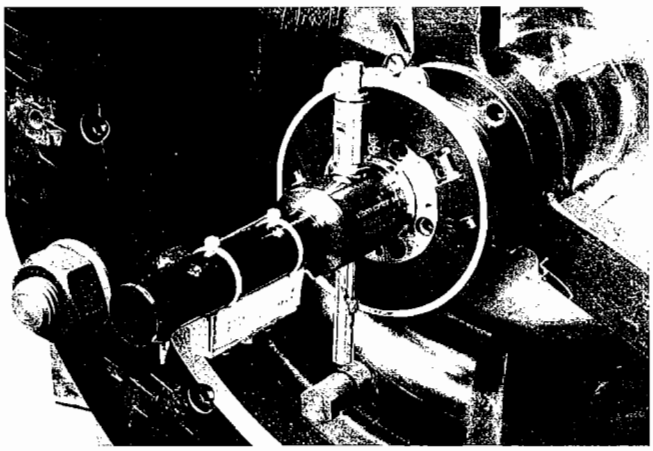

Figure 2. Angular Acceleration Sensor and Transmitter.

TEST PUMP

The test pump is a single stage pump (Figure 3) with radial impeller and diffuser. It represents the inlet chamber and the suction stage of a multistage pump. The shaft is supported in two antifriction bearings. The pump had originally been built for cavitation observation tests.

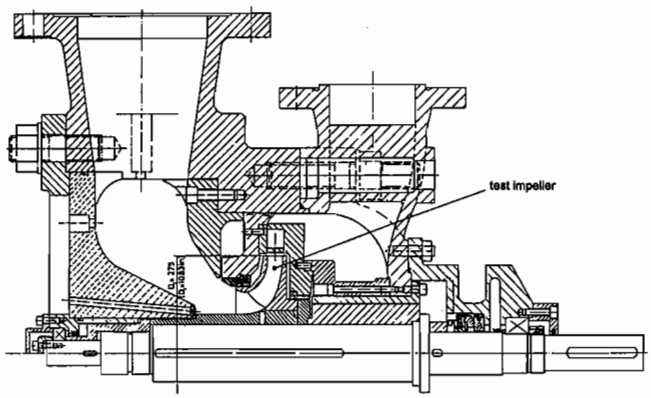

Figure 3. Test Pump

IDENTIFICATION PROCEDURE

The coherence between the damping and mass parameters of the impeller and the input torque is represented by the differential equation governing the transfer characteristics of the system. The input torque is measured using a torque measuring shaft while the angular acceleration is registrated using the acceleration sensor (Figure 4).

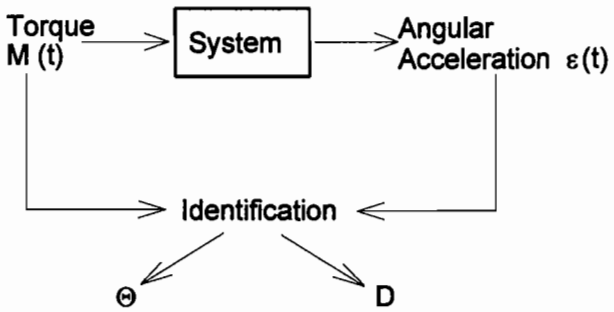

Figure 4. Input and Output Parameters.

The system consisting of impeller and flow medium can be regarded as a damped, single-mass torsional vibration system.

Additionally, there are no elastic couplings between the fluid and the housing. Assuming that the damping torque is proportional to the angular velocity of the shaft, then the system can be described by:

$$\Theta \ddot{\varphi}(t) + D \dot{\varphi}(t) = M(t) \tag{6}$$

with

	Θ	mass moment of inertia (kg/m²)
	D	damping (Nms)
	M (t)	torque (Nm)
	φ (t)	rotational angle (rad)

With the solution

$$\varphi(t) = \underline{\hat{\varphi}}\, e^{i\Omega t} \tag{7}$$

and the impedance function:

$$H = \frac{M(t)}{\varphi(t)} \tag{8}$$

and the equation for the torque

$$M(t) = \underline{\hat{M}}\, e^{i\Omega t} \tag{9}$$

the following is obtained

$$-\Omega^2 \Theta + i\Omega D = \frac{\hat{M}}{\underline{\hat{\varphi}}} \tag{10}$$

The moment and damping parameters can be extracted from the real and imaginary part of the impedance function. Due to the fact that the sensor is measuring the angular acceleration, substitute the amplitude of the angular velocity and finally obtain:

$$\Theta - i\,(D/\Omega) = \frac{\hat{M}}{\underline{\hat{\varepsilon}}} = H^* \tag{11}$$

$$\text{with } \hat{\varepsilon} = \underline{\hat{\ddot{\varphi}}}$$

From this equation it can be clearly seen, that the mass moment of inertia is equal to the real part of the impedance function while the damping can be calculated from the imaginary part:

$$\Theta = \mathrm{Re}\left\{H^*\right\} \tag{12}$$

$$D = -\Omega\, \mathrm{Im}\left\{H^*\right\}$$

The complex amplitudes of torque and angular acceleration can be calculated from the time signals of torque measurement shaft and angular acceleration sensor using FFT. In practice, this is done using a spectral analyzer (Figure 5). Because the amplifier in the torque measuring chain imposes a phase change to the signal, the differential measurement principle had to be adopted:

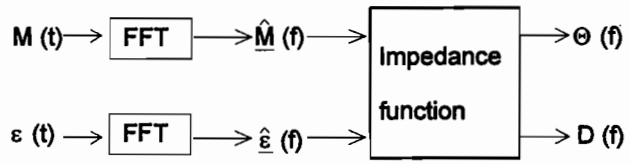

Figure 5. FFT Procedure to Obtain Dampng and Mass Moment.

- A first measurement is done with the pump running in air. The measured impedance function H_{air} is stored in the computer.
- A second measurement is done with the pump running in water. The impedance function H_{water} is alsostored in the computer.
- The vector difference

$$H_{eff} = H_{water} - H_{air} \quad (13)$$

is the effective impedance due to the influence of the water.

With this method, two aims can be achieved at once:

- Phase changes are eliminated
- Contributions from bearings and shaft seals are eliminated.

Signal conditioning (curve smoothing) had to be done before the above vector difference could be built.

TEST RESULTS–COMPARISON WITH THEORETICAL PREDICTIONS

Two different pump stages with specific speeds nq of 22 (m3/s, m) (1130 (gpm, ft)) and 33 (m3/s, m) (1700 (gpm, ft)) have been investigated in the test rig. Pump running speed was 1500 rpm.

The results are shown on diagrams Figure 6, 7, 8, and 9. Damping and added mass moment of inertia have been measured at five different load points: 25, 50, 75, 100, and 125 percent of best efficiency flow, and plotted against the vibration frequency. A strong dependence on vibration frequency can be observed. Apparently, the damping curves drop to zero at zero frequency.

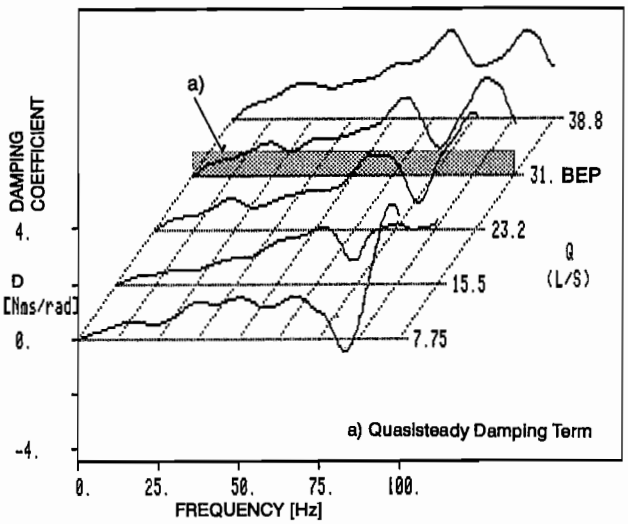

Figure 6. Damping Coefficient for n_q 22 Impeller as a Function of Load and Ferquency.

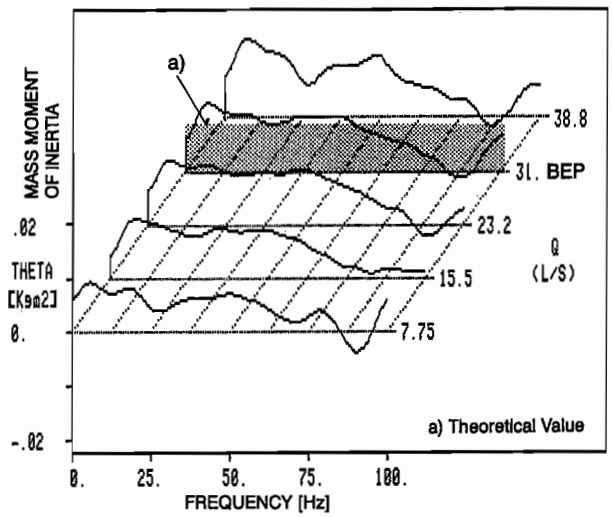

Figure 7. Added Mass Moment of Inertia for n_q 22 Impeller as a Function of Load and Ferquency.

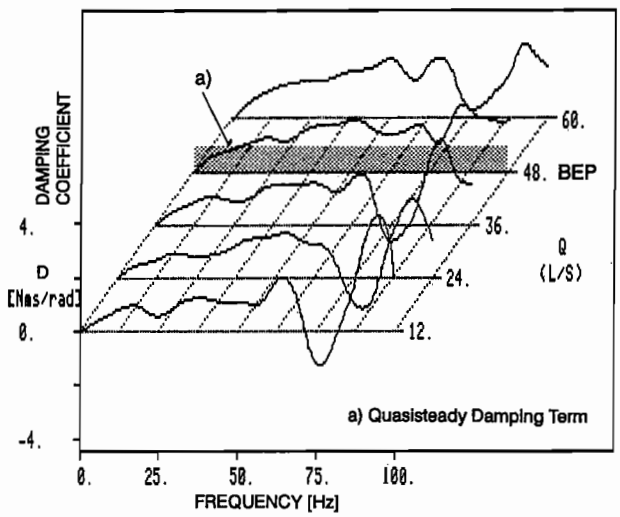

Figure 8. Damping Coefficient for n_q 33 Impeller as a Function of Load and Ferquency.

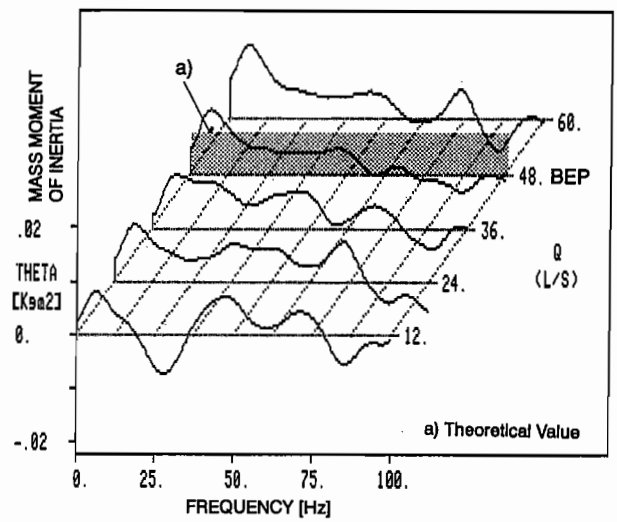

Figure 9. Added Mass Moment of Inertia for n_q 33 Impeller as a Function of Load and Ferquency.

However, this is rather a problem with the identification procedure than real physical behavior. In reality, the damping coefficient is expected to approach the quasisteady damping term according to Equation (5) when the frequency approaches zero. The quasisteady damping term as an average fits quite well with the measured damping curves at best efficiency flow.

The effective added mass moment of inertia can be written

$$\theta_{eff} = C_\theta \, \theta_{Channel} \tag{14}$$

where $\theta_{Channel}$ is the mass moment of inertia of the fluid within the impeller channels as shown in Figure 10 and C_θ gives the percentage that takes part in the vibration. According to Imaichi, et al. [5], C_θ is a function of the ratio inner to outer diameter, the vane angle, and the number of vanes as shown on the diagrams Figure 11. For the two impellers investigated, C_θ taken from the above diagrams is about 0.6.

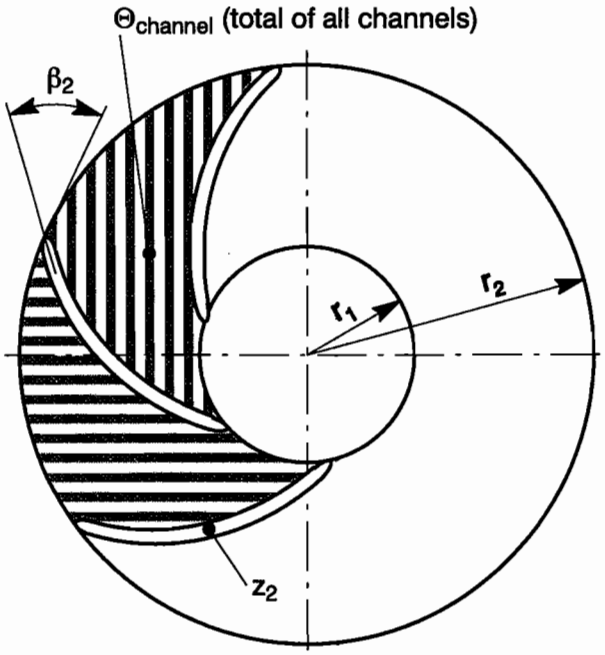

Figure 10. Definition of $\Theta_{channel}$.

However, the measurements indicate a strong dependence of θ_{eff} on vibration frequency. For low specific speed impellers, this is of little practical relevance, because the fluid mass moment of inertia is only a small fraction of that of the impeller. Thus, the torsional natural frequencies are hardly influenced by the liquid pumped. For high specific speed impellers, the situation is different.

θ_{eff}, according to Equation (14) as an average fits quite well with the measured distribution at least near best efficiency flow and for a lower frequency range up to two times running speed frequency.

However, there are frequency regions, especially at part load where damping and added mass term are negative. Similar phenomena are known for the lateral vibration behavior of tubes with a fluid flow across the tubes [9]. Hence, external damping from impellers has to be handled with care in torsional rotordynamic analysis. According to the experimental results shown on diagrams Figures 6 and 8, an impeller damping calculated with Equation (5) can be used with confidence for frequencies up to four times running speed (1×) frequency, near best efficiency flow.

A comparison between the measured damping curves for best efficiency flow and a theoretical curve derived from the investigation of Imaichi, et. al. [5], is shown in Figure 12. The theoretical curve contains not only the quasisteady term, but also the wake

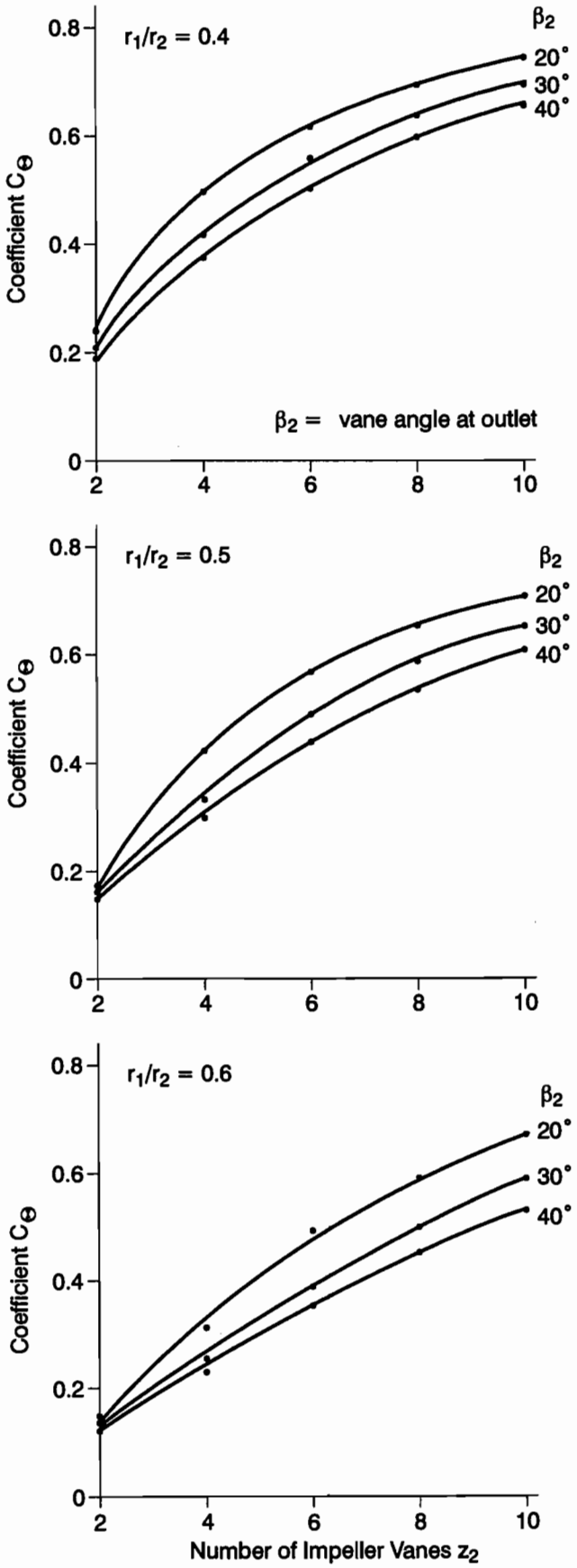

Figure 11. Coefficient C_Θ for the Added Mass Moment of Inertia.

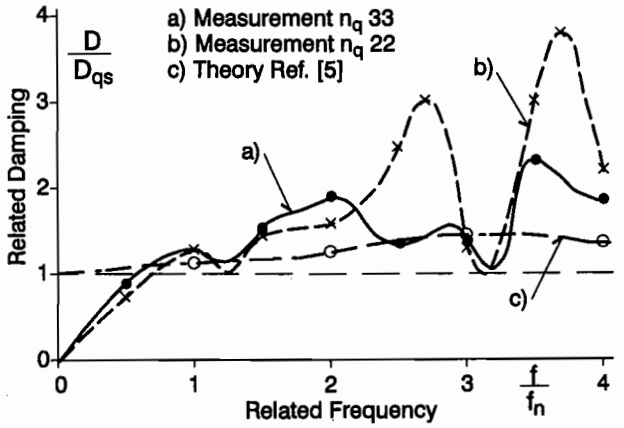

Figure 12. Comparison Measured vs *Theoretical Damping. D_{qs} = quasisteady damping term; f_n = shaft speed frequency = n/60.*

term due to alternating vortex shedding at the trailing edge of the impeller vanes. Obviously, the theory applied does not explain the heavy fluctuation of the experimentally determined damping with frequency.

APPLICATION ON A PUMP SHAFT TRAIN WITH VARIABLE SPEED ELECTRIC MOTOR

The pump set investigated consists of a variable speed motor with speed control of the subsynchronous converter cascade type [2], a speed increasing spur gear, and a pump of the double entry type with two stages as shown in Figure 13. The layout of the pumpset is shown in Figure 14. Main data are given in Table 2. The pumpset is used for drinking water transport.

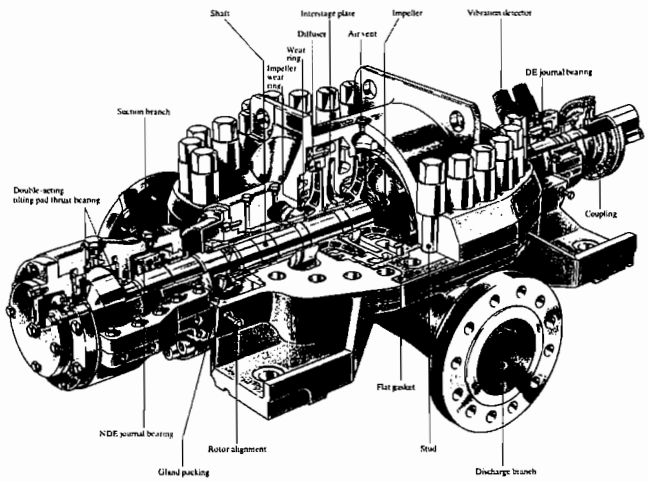

Figure 13. Horizontally Split Casing Pump, Type HPDM.

Torsional vibration behavior, in contrary to lateral behavior, is typically not monitored on pumpsets. Sophisticated instrumentation is needed to measure torsional vibration. Such instrumentation is used at present only for R&D purposes. Hence, the acceptability of a shaft train with respect to its torsional behavior has to be based on a reliable torsional analysis. This is of utmost importance if resonance situations cannot be avoided, as explained in the preceding sections.

Through the influence of the subsynchronous converter cascade, the electric motor produces, besides a nonpulsating static torque, a pulsating torque whose frequency f_{ex} is proportional to the slip S:

$$f_{ex} = 6\ S\ f_{line} \tag{15}$$

$$s = \frac{n_{syn} - n}{n_{syn}} \tag{16}$$

pulsating torque component can therefore be written

$$M(t) = M_6(n)\ \sin(2\pi f_{ex}\ t) \tag{17}$$

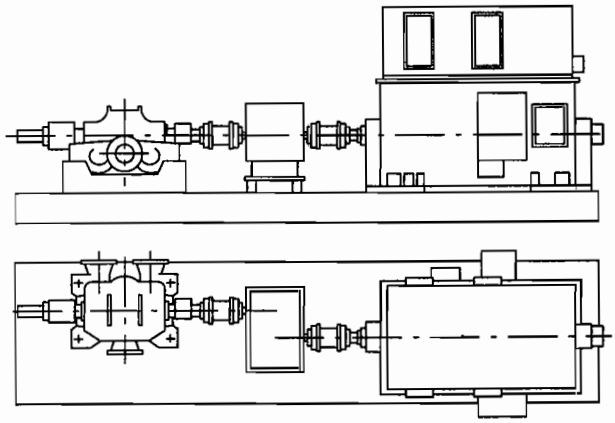

Figure 14. Pump Set Layout.

Table 2. Pump and Motor Data.

Impeller Diameter	[mm]	380
	[in]	15
Rated Pump Head	[m]	477
	[ft]	1565
Rated Pump Flow	[m3/s]	0.513
	[gpm]	8132
Rated Pump Power	[kW]	2762
Rated Pump Speed	[rpm]	3580
Rated Pump Torque	[Nm]	7367
Motor Power	[kW]	3500
Synchr. Motor Speed	[rpm]	1800
Gear Ratio	[-]	2.053

The first part of the analysis consists of a damped natural frequency calculation. The model of the shaft train is shown in Figure 15. Mode shapes, natural frequencies, and modal damping rates

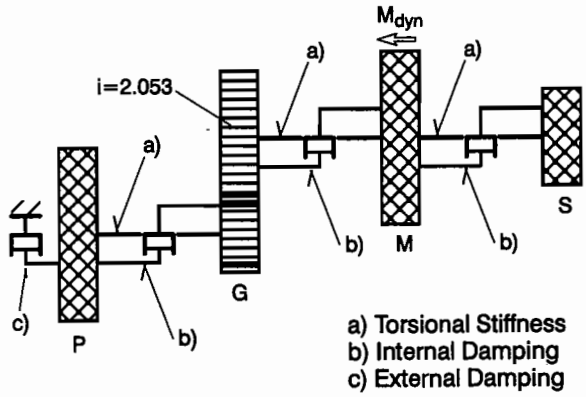

Figure 15. Model for Torsiomal Analysis P = Pump, G = Gear, M= Motor, S = Slipring.

(critical damping ratio) for the first three modes are presented in Figure 16. The internal damping has been adjusted by selecting a damping term proportional to stiffness such that the critical damping ratio of the first mode at 37.9 Hz is one percent. When keeping this proportional damping term, the second and third mode have higher critical damping ratios. The contribution from external impeller damping is speed dependent. The modal damping rates shown in Figure 16 are valid for the maximum pump speed of 3580 rpm.

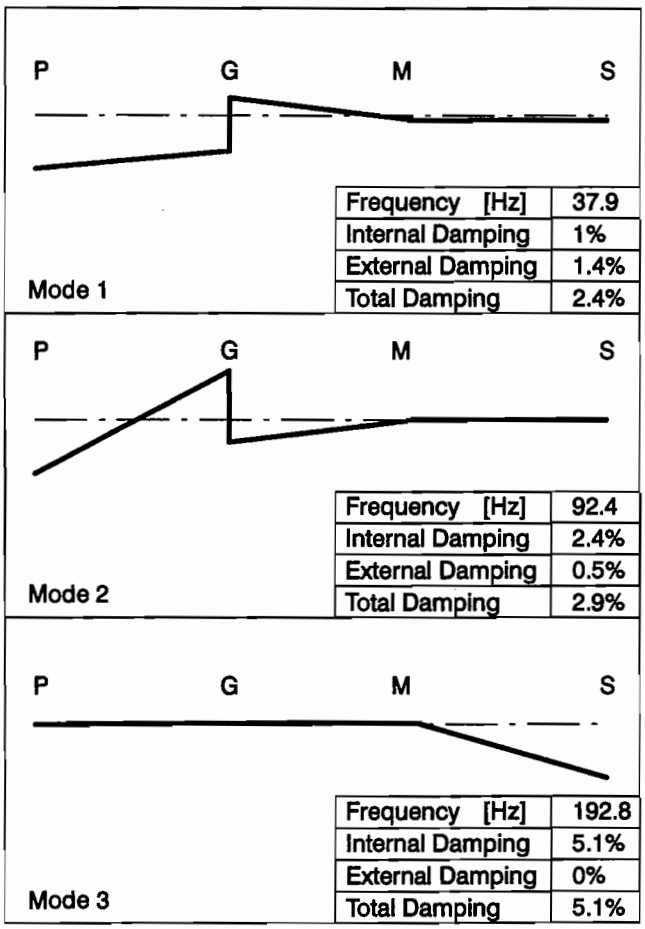

Figure 16. Eigenvalves and Mode Shpes P = Pump, G = Gear, M= Motor, S = Slipring.

The first mode will be in resonance with the pulsating torque according to Equation (17) at a pump speed of 3307 rpm, where the excitation frequency according to Equation (15) is equal to the first natural frequency at 37.9 Hz, (Figure 17). For the second mode, this resonant speed is at 2746 rpm.

The second part of the analysis is a steady state harmonic excitation analysis with the forcing function as given in Equation (17). The amplitude $M_6(n)$ of the pulsating torque component calculated by the motor supplier is 1800 Nm for rated condition. It is basically a function of speed; however, it was kept constant which is a conservative assumption. The results of this analysis are summarized in Table 3. The rotor response at the resonance conditions has been determined via a frequency sweep across the resonance as shown in Figure 18 for resonance with the first mode. The introduction of impeller damping reduces the dynamic torque by a factor of 2.4 for the first mode. The second mode is hardly excited; the mode shape of the second mode shows virtually no displacement at the motor location.

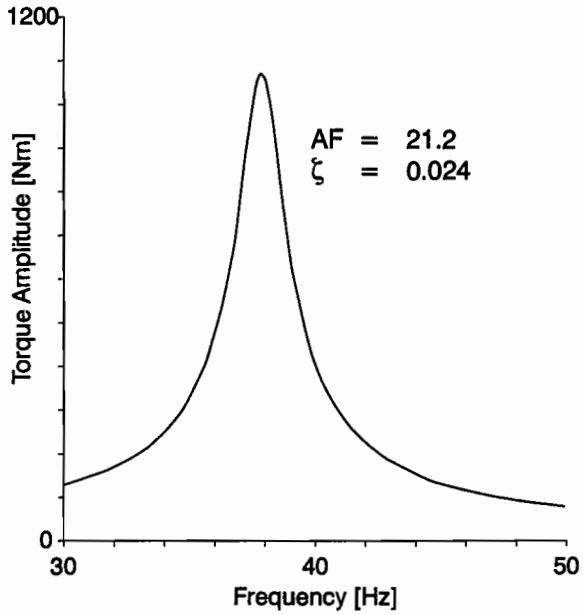

Figure 17. Campbell Diagram.

Table 3. Results for Steady-State Excitation at Resonance.

Resonant Mode			1	2
Frequency		[Hz]	37.9	92.4
Pump Speed		[rpm]	3307	2747
Rated Torque	M_r	[Nm]	7367	7367
Dyn. Torque $\hat{M}$ Gear-Pump				
• Internal Damping only		[Nm]	2554	176
Ratio	$\hat{M}/M_r$	[-]	0.35	0.024
• Internal + External Damping		[Nm]	1075	152
Ratio	$\hat{M}/M_r$	[-]	0.15	0.021
Motor Speed		[rpm]	1611	1338
Rated Torque	M_r	[Nm]	15124	15124
Dyn. Torque $\hat{M}$ Motor-Gear				
• Internal Damping only		[Nm]	10768	158
Ratio	$\hat{M}/M_r$	[-]	0.71	0.010
• Internal + External Damping		[Nm]	4478	140
Ratio	$\hat{M}/M_r$	[-]	0.30	0.009

The following question arises: What percentage of the nonpulsating torque can be allowed for the pulsating torque amplitude without the need to perform an indepth fatigue failure analysis?

If the following conservative assumptions are taken

- Fatigue notch factor $\beta_f = 3$
- Fatigue (endurance) limit $\tau_f = 0.5\ \tau_y\ (1-\tau_{np}/\tau_y)$
  τ_y = Yield strength (shear)
  τ_{np} = Nominal shear stress due to nonpulsating torque
- Safety factor against fatigue failure = $SF_f = 2$
- Safety factor against gross yielding = $SF_y = \tau_y/\tau_{np} = 3$

a ratio

$$\frac{M_p}{M_{np}} = \frac{\tau_p}{\tau_{np}} = \frac{0.5\tau_y(1-\tau_{np}/\tau_y)SF_y}{\beta_f SF_f \tau_y} \le 0.16 \qquad (18)$$

yields. Hence, if the pulsating torque amplitude in a shaft section is not higher than about 16 percent of the rated nonpulsating torque, no danger of a fatigue failure exists, provided the shaft has been properly sized and designed with respect to its notch radii, and a shaft material withstanding any possible corrosion attack has been selected.

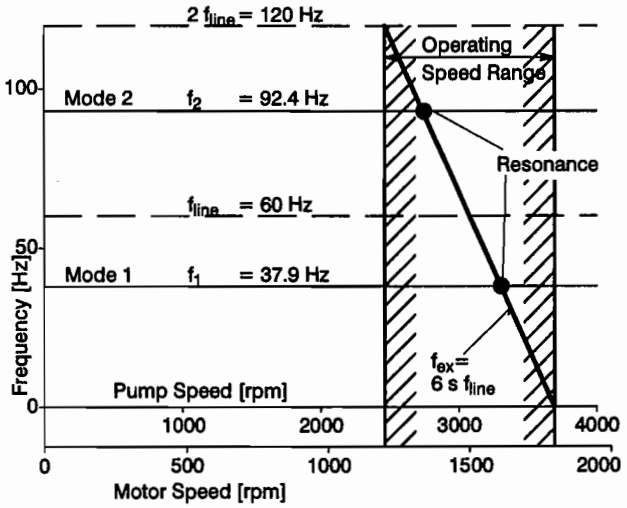

Figure 18. Calculation of Torque Response at Resonance.

Referring to the numbers shown in Table 3, the shaft train section between gear and pump can be considered safe with respect to high cycle fatigue, without a detailed assessment of each stress raising element, when impeller damping is taken into account; the shaft train section between motor and gear however has required a careful evaluation of all peak stresses to assure a safe running at the resonant speeds for extended time periods.

At startup, the shaft train is also subject to a transient dynamic excitation. When the motor is switched to the line, a transient torque which is described by the following Equation develops in the airgap of the motor:

$$M(t) = M_0(1-e^{-t/T1}e^{-t/T2}) + M_1 e^{-t/T1}\sin(2\pi ft-\alpha) - M_1 e^{-t/T2}\sin(2\pi ft+\alpha) \quad (19)$$

A graph of this function for the case investigated is shown in Figure 19. Excitation frequency is equal to line frequency which is 60 Hz. The transient dynamic torques developing between motor and gear and between gear and pump are shown in Figures 20 and 21. The maximum torque values have to be compared with the nominal (rated) torque transmitted which is 15124 Nm, between motor and gear and 7367 Nm between gear and pump. Thus,

- Between motor and gear $M_{peak}/M_{rated} = 7572/15124 = 0.50$
- Between gear and pump $M_{peak}/M_{rated} = 2320/7367 = 0.31$

A shaft train has to be designed related to nominal torque with a safety factor of three against gross yielding as the very minimum. Hence, the above peak torques can be taken by the shaft train without any danger of gross plastification or distortion. Another question is the number of starting transients allowable without any danger of low cycle fatigue failures at locations with high peak stresses.

For the transient excitation at startup, rotor damping in the case investigated has little influence on the dynamic torque along the train, because the excitation frequency is far from any torsional

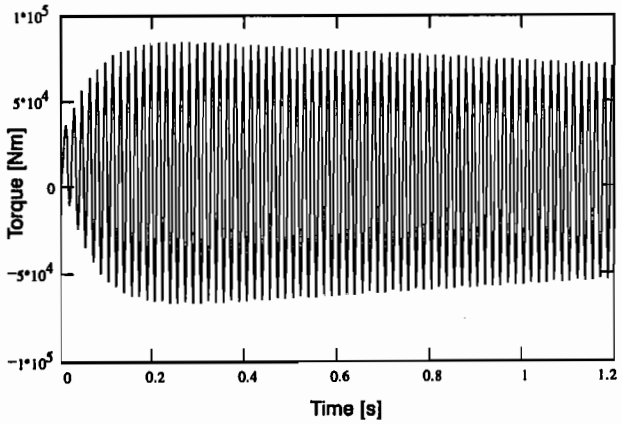

Figure 19. Airgap Torque during Motor Startup.

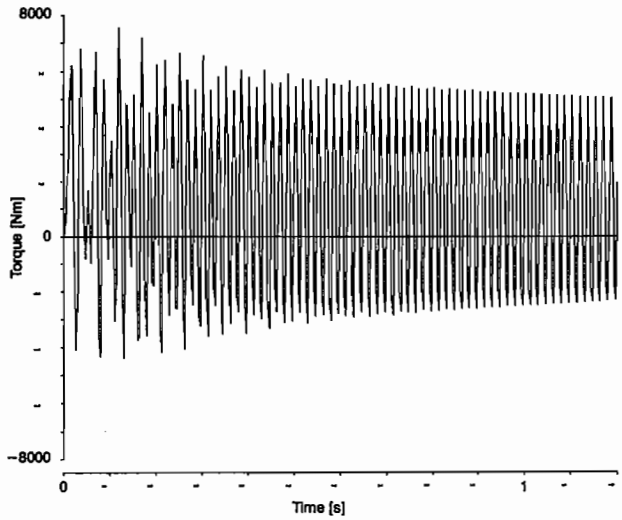

Figure 20. Torque between Motor and Gear.

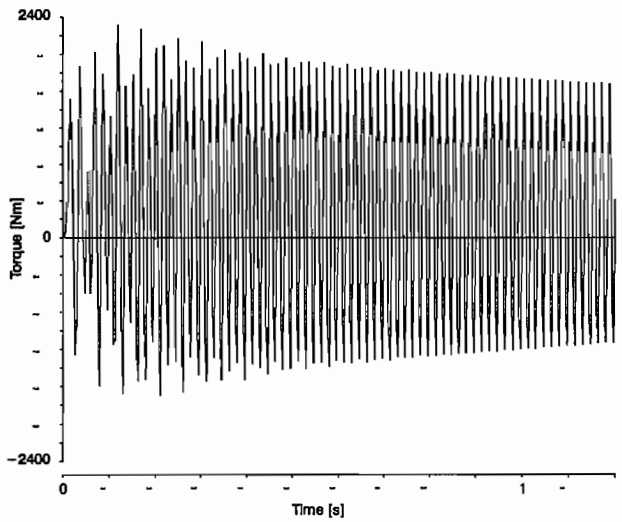

Figure 21. Torque between Gear and Pump.

natural frequency. However, if resonance occurred, the amount of damping available would again be the determining parameter influencing the rotor response for a given excitation.

Transient torque amplitudes in the airgap of the motor at startup or during electrical faults like phase-to-phase terminal short circuit are very high when compared with the nominal torque. The ratio peak torque to rated torque ranges from four to values beyond ten. Excitation frequencies are stator feed (line) frequency for startup and short circuit, and additionally twice stator feed frequency for short circuit, as shown in Table 1. Whenever possible, torsional natural frequencies should be separated from the above two excitation frequencies by at least 20 percent. If this is not possible, which is the case, e.g., for synchronous thyristor controlled variable speed motors, where the stator feed frequency is proportional to speed and, hence, variable [2], the behavior at resonance has to be carefully investigated.

Also, for constant speed asynchronous motors directly switched to the line, the behavior at startup should be investigated, even in a nonresonant case, if the mass moment of inertia of the driven components (gear, pump) reduced to the driver shaft, Thompson [8], is more than about 30 percent of that of the motor.

CONCLUSIONS

Based on the findings presented in this paper the following conclusions can be drawn:

- The interaction between impeller vanes and fluid pumped on a torsionally vibrating pump rotor results in an added mass moment of inertia and in torsional damping.
- Measurements carried out on a test rig have shown that added mass moment of inertia as well as damping depend strongly on the vibration frequency.
- A reasonably conservative approximation for the torsional damping term near best efficiency flow and for a frequency range from zero up to about four times running speed frequency is given by the quasi steady damping term as defined in section three of this paper.
- An approximation for the added mass term can be given as a percentage of the mass moment of inertia of the fluid contained in the channels between the impeller vanes.
- The damping from the impellers can considerably reduce the amplification factor at resonance such that a continuous run at a resonance between a torsional natural mode and an excitation by a variable speed electric motor is possible. However, every case has to be investigated and judged individually.
- During startup and at an electrical fault condition like a phase-to-phase short circuit, high transient torque pulsations develop in the airgap of electric motors. The frequencies of these transient torque pulsations are located at one and two times stator feed frequency. Resonance with these frequencies shall be avoided whenever possible.
- Further experimental and theoretical work needs to be done to clarify the dynamic torsional behavior of an impeller with respect to load and vibration frequency.

NOMENCLATURE

AF		Amplification factor
C		Constant
D	(Nms)	Damping coefficient
e		Basis for natural logarithm
f	(Hz)	Frequency
H		Impedance function
i		Imaginary unit
M	(Nm)	Torque
n	(rpm)	Shaft speed
n_{syn}	"	Synchronous shaft speed
P	(W)	Power
SF		Safety factor
t	(s)	Time
T	(s)	Time constant
α	(rad)	Phase angle
β		Fatigue notch factor
ε	(s^{-2})	Angular acceleration
φ	(rad)	Rotational angle
Θ	(kgm^2)	Mass moment of inertia
τ	(N/m^2)	Shear stress
ω	(s^{-1})	Shaft angular speed
Ω	(s^{-1})	Vibration angular frequency
ζ		Critical damping ratio

REFERENCES

1. Wolff F.H. and Molnar A. J., "Variable-Frequency Drives multiply Torsional Vibration Problems," Power (1985).
2. Frei, A., et al., "Design of Pump Shaft Trains having Variable-Speed Electric Motors," *Proceedings of the Third International Pump Users Symposium,* Turbomachinery Laboratory, Texas A&M University, College Station, Texas (1986).
3. Vance, J. M., *Rotordynamics of Turbomachinery,* New York, New York: John Wiley & Sons (1987).
4. Ehrich, F. F., *Handbook of Rotordynamics,* New York, New York: Mc Graw-Hill (1992).
5. Imaichi, K., et al, "An Analysis of Unsteady Torque on a two-dimensional Radial Impeller," ASME Journal of Fluids Engineering (1982).
6. Tsujimoto, Y., et al, "A two-dimensional Analysis of Unsteady Torque on Mixed Flow Impellers," ASME Journal of Fluids Engineering (1986).
7. Bolleter, U., "Blade Passage Tones of Centrifugal Pumps," Vibrations, *4* (3), (1988).
8. Thomson, W. T., *Theory of Vibration with Applications,* Englewood Cliffs, New Jersey: Prentice Hall Inc. (1981).
9. Sarpkaya, T., "Vortex-Induced Oscillations," ASME Journal of Applied Mechanics, *46* (1979).